Visibility Laboratory
University of California
Scripps Institution of Oceanography
San Diego 52, California

CORRELATION BETWEEN MEASURED PATH FUNCTION AND RELATIVE HUMIDITY

Almerian R. Boileau

1 February 1959
Index Number NS 714-100

Bureau of Ships
Contract NObs-72092

SIO REFERENCE 59-5

Approved:

Seibert Q. Duntley, Director
Visibility Laboratory

Approved for Distribution:

Roger Revelle, Director
Scripps Institution of Oceanography

Correlation Between Measured Path Function and Relative Humidity*

Almerian R. Boileau

Scripps Institution of Oceanography, University of California

La Jolla, California

INTRODUCTION AND SUMMARY

The Visibility Laboratory of the University of California, La Jolla Campus, is engaged in an on-going research program studying image transmission through the atmosphere. The paper "Image Transmission by the Troposphere I,"[4] published in the Journal of the Optical Society of America, discusses this program. In that paper correlation between certain optical and meteorological parameters is indicated. The study of this correlation has continued and this report describes the results of data gathered from a second formation flight of two airplanes, the instrumented B-29 and a microwave refractometer-equipped C-131 from Patrick Air Force Base squadron.

It was found that when the relative humidity is high, approximately 85 percent and higher, small changes in relative humidity are accompanied by large changes of path function, i.e., the scattering of radiant flux from particles in the air; when the relative humidity is approximately 60 percent or lower, large changes in relative humidity are accompanied by small changes of path function; and in the range of relative humidities from 65 percent to 85 percent a more complicated relationship between relative humidity and path function exists.

---

* This paper represents results of research which has been supported by the Bureau of Ships, U. S. Navy and the Geophysics Research Directorate, Air Force Cambridge Research Center, Bedford, Massachusetts.

PROCEDURE

On 6 May 1957 the B-29 and C-131 took off from Patrick Air Force Base at approximately 1330 E.S.T. The two airplanes were taken to 18,000 feet altitude. During this ascent a record of air temperature was made. At 1436 E.S.T. at 18,000 feet, a descent was started in which the two airplanes, flying in formation, maintained a descent rate of approximately 1000 feet/minute. In the descent the B-29 was held in a level attitude (indicated by a bubble level attached to the pilot's aisle stand), with the power reduced and landing gear extended to increase drag. During the descent the temperature and the optical parameters for which the B-29 and the microwave refraction modulus for which the C-131 is instrumented was recorded in the C-131. The descent ended at 500 feet at 1509 E.S.T. The records of all parameter values are continuous as a function of altitude.

INSTRUMENTATION

The parameters referred to in this report are listed below together with their symbols and instrumentation:

Temperature, Centigrade	t	Measured by ML-471/AMQ-8 indicating resistance thermometer. This instrument measures accurately to $\pm$ 0.5°C, and reproduces its indication at $\pm$ 0.1°C.
Temperature, Absolute	T	$t^{\circ}C + 273.15^{\circ}$
Total pressure, atmospheric	p	Millibars. Obtained from B-29 altimeter.
Microwave refractive modulus	N	"N units." Measured by University of Texas type microwave refractometer installed in C-131.
Relative humidity	e/e_s	Computed from N, T, and p.
Path function	$B_*(z,\theta,\phi)$	Foot lamberts per nautical mile. Measured by attenuation meter mounted on B-29 fuselage. The parenthetical subscripts are: z - altitude in feet θ - zenith angle of line of sight ϕ - azimuth angle of line of sight and sun's bearing
	${}_{\Lambda}B_*(z,\theta,\phi)$	For pure, dry air. Foot lamberts per nautical mile. Computed.
	${}_{p}B_*(z,\theta,\phi)$	For particles in suspension. Foot lamberts per nautical mile. ${}_{p}B_* = B_* - {}_{\Lambda}B_*$

Volume Scattering Function	$\sigma_\lambda(z; \phi')$	For unit length. This is a function of altitude, z; the angle between incident and scattered flux, ϕ', and wave length λ .
Volume attenuation function	$\alpha(z)$	Per unit length. This is a function of z(altitude). It is the sum of s(z), the total scattering function, and a(z), the volume absorption function.
Total scattering function	s(z)	Per unit length. This is a function of altitude. It equals the integral $\int_{4\pi} \sigma(z; \phi') d\Omega$

DISCUSSION

Immediately after take-off from Patrick A.F. Base the B-29 and C-131 climbed to altitude. During this ascent to station altitude the ambient air temperature was recorded at one hundred feet intervals and visual observations of the sky were recorded. The temperature plot as a function of altitude is shown in Fig. 1. Added to the graph are notes regarding observed clouds and haze layers. Overlaid on the graph are solid lines which represent temperature lapse of saturated air, often referred to as "wet adiabats."

Fig. 2 shows the temperature profile recorded during descent from 18,000 feet to 8,000 feet, and from 8,000 feet to 500 ft. A comparison of these two temperature profiles is of interest:

Differences Between Temperature Profiles for Ascent and Descent.

The ascent profile shows more fine structure than the descent profile. This should not be given too much importance for the following reason: The ascent was from 1336 to 1424, a time lapse of 48 minutes; the descent from 1436 to 1457, and from 1501 to 1509, periods of 15 and 8 minutes respectively, or total of 23 minutes. Thus it is seen that during the ascent the airplane covered at least twice the horizontal distance than it did during descent. Now it is known that the atmosphere is not homogeneous in that there are moisture cells present. These cells are left after small cumulus clouds have evaporated, and represent a greater concentration of water vapor than the air surrounding them. They may be several hundreds of feet thick. Thus an airplane climbing at a rate of approximately 300 ft/min at a forward speed of

150 knots or better, upon reaching a stratum of moisture cells might easily pass through several of these cells in succession while climbing through the stratum. (This is illustrated in Fig. 3). If there are temperature differences inside and outside of the cells the record would show the effect of each cell as the airplane continues its climb, and this might be interpreted as the airplane having gone through several temperature inversions. This is, of course, in error. Accordingly, the temperature recorded during descent is considered to be more representative of the true air temperature pattern.

During descent the temperature was recorded as being lower, generally, than during ascent. The descent started 12 minutes after arrival on station, it terminated 1 hour and 33 minutes after start of climb following take-off, the elapsed time being in mid-afternoon with the sun's zenith angle increasing toward the west. This would indicate that the temperature was in fact lowering. However, the shape of the descent profile at 18,000 ft. to 17,500 ft., i.e., a comparatively small change of temperature with altitude, may indicate a lag in altimeter readings. The fact that the inversion near 7,000 ft. is recorded approximately 200 ft. lower during descent might be interpreted as confirming an altimeter lag. However, because all data recorded during descent are correlated to that one parameter, the altimeter altitude, the effect of the error is minimal. Accordingly, the temperature recorded during descent has been used for all data reduction. Data recorded in the C-131 were synchronized with the B-29 data by voice radio.

Microwave Refractive Modulus. Fig. 4 is a plot of microwave refractive modulus as a function of altitude, and the corresponding relative humidity computed from microwave refractometer and other data. The microwave refractive modulus[4] is defined as follows:

$$N = (n-1)\ 10^6 \qquad (1)$$

where n is refractive index of air. A typical value of the refractive index of air of 1.000300 is indicated as microwave refractive modulus of 300, often referred to as 300 "N units." The microwave refractometer measures N directly. Then by using the recorded centigrade temperature converted to absolute temperature and the atmospheric pressure corresponding to altimeter altitude, the partial pressure of water vapor, e , in millibars, is computed[4] from the following Debye equation:

$$N = \frac{77.6\,p}{T} + \frac{77.6 \times 4810\,e}{T^2} \qquad (2)$$

where N is in "N units," T is absolute temperature, and p is total atmospheric pressure in millibars.

Determination of Relative Humidity. By setting e = o , the second term of the right hand side of the above equation is zero, and $N = \frac{77.6\,p}{T}$. This is the equation of microwave refractive modulus for dry air. This is plotted in Fig. 4, as the farthest to

the left. By setting $e = e_s$, the partial pressure of water vapor at dew point temperature, the equation is

$$N = \frac{77.6\,p}{T} + \frac{77.6 \times 4810}{T^2} e_s$$

and the plot of this equation shows the microwave refractive modulus for saturated air. The microwave refractive modulus for the ambient air, if the air is not completely dry or saturated, must fall between the two limiting curves. This it does.

Now the difference between the left limiting curve and recorded N unit curve is $\frac{77.6 \times 4810}{T^2} e$, and the difference between the two limiting curves is $\frac{77.6 \times 4810}{T^2} e_s$. Thus the ratio of these two quantities is e/e_s, the approximate relative humidity.

Relative humidity is defined[8] as the ratio of observed and saturated mixing ratios, the mixing ratios being:

$$\text{observed} - \frac{.622\,e}{p - e}$$

$$\text{saturated} - \frac{.622\,e_s}{p - e_s}$$

The ratio $\frac{.622e}{p-e} \Big/ \frac{.622\,e_s}{p-e_s}$ reduces to $\frac{e}{e_s} \times \frac{p-e_s}{p-e}$, but because e and e_s are very small compared to p, $\frac{p-e_s}{p-e} \doteq 1$ and relative humidity $\doteq e/e_s$.

Relative Humidity vs Altitude. The plot on the right side of Fig. 4 is relative humidity computed as a function of altitude. A comparison of the relative humidity with the observed clouds and haze layers indicated on Fig. 1, shows that the clouds at 3500-6000 feet correspond to high relative humidity, and the haze layer at 13000 feet corresponds to another stratum of increased humidity.

Path Function vs Altitude. Also recorded during descent was the path function, $B_*(z,\Theta,\emptyset)$. (In this report the notation for path function $B_*(z,\Theta,\emptyset)$ indicates the photopic case while $N_*(z,\Theta,\emptyset)$, used in reference 4, indicates the general radiometric case.) The path function, a measure of the light flux being scattered from a volume of aerosol, is dependent on two things, the character of the illumination, and the character of the aerosol. If the geometry and intensity of the illumination remain constant, a change in the value of the path function indicates a change in the character of the aerosol.

During a change of altitude, if the character of the aerosol and geometry of lighting remain constant, there will be a regular change of path function due to the change in density of the aerosol, the path function at altitude being related to the path function at sea level by the equation

$$B_*(z,\Theta,\phi) = B_*(0,\Theta,\phi)\, e^{-z/k} \qquad (3)$$

where e is the natural logarithmic base, z is altitude in feet, and k is the altitude in feet at which the path function at that altitude is 1/e of path function at sea level. This altitude is approximately 30,000 feet. This is one of the factors which characterizes the "Optical Standard Atmosphere."[14]

In addition to the exponential change of B_* due to change of air density there will be another change due to change in the character of the aerosol. This is shown in Fig. 5. Plotted farthest to the left is the ${}_AB_*(z,90^\circ,90^\circ)$ value as a function of altitude for pure dry air. This was computed as follows:

Computation of Path Function for Dry Air. Tousey and Hulburt[15] have defined the "optical scattering coefficient" by the equation

$$i_{\phi\lambda} = \sigma_{\phi,\lambda} \; \iota_\lambda$$

In the notation used in this report the above equation is

$${}_AN_{*\lambda}(z,\theta,\phi) = \sigma_\lambda(z;\phi') \times H_\lambda \qquad (4)$$

where ${}_AN_{*\lambda}$ (z,θ,ϕ) is radiance value of electro-magnetic radiation of wavelength λ being scattered at altitude z, zenith angle θ, and solar azimuthal angle ϕ; $\sigma_\lambda(z;\phi')$ is the volume scattering function for wavelength λ at altitude z, and angle between incident flux and scattered flux of ϕ'; and H_λ is the irradiance of

wavelength λ incident on the scattering volume. The volume scattering function for the case of Rayleigh scattering is further defined as[15]

$$\sigma_\lambda(0;\phi') = \frac{2\pi^2}{N\lambda^4}(m-1)^2(1+\cos^2\phi') \qquad (5)$$

where m is index of refraction of air; N is Loschmidt's number 2.687×10^{19}, the number of molecules per cm^3 of an ideal gas at standard atmospheric pressure and 0°C; λ is wavelength; and ϕ' is the scattering angles as defined above. Note that $\sigma_\lambda(0;\phi')$ is now limited to an altitude of z = o, i.e., sea level. The ${}_AB_*$, or luminance value of path function, the total scattered radiance per cm^2 per steradian, at sea level, at zenith angle of 90°, and solar azimuth angle of 90° (i.e. $\phi' = 90°$), across the visible spectrum was found by Eq (5) as follows:

$${}_AA_*(0,90°,90°) = 680\frac{2\pi^2}{N}(m-1)^2\sum_{400}^{700} S_\lambda T_\lambda \frac{H\lambda}{1000}\lambda^{-4}\Delta\lambda \times F$$

where 680 is the luminous efficiency term; $S_\lambda T_\lambda$, the normalized product of spectral sensitivity of phototube and spectral transmittance of filter (ideally this is equal to $\bar{y}$, the luminous efficiency factor as a function of wavelength, but in this case $S_\lambda T_\lambda$ is the real value for the phototube-filter combination, being slightly different than $\bar{y}$.); $H\lambda$ the solar irradiance outside the earth's

atmosphere in watts cm^{-2} u^{-1} as tabulated by Johnson[10]; λ is wavelength in cm; $\Delta\lambda$ bandwidth of 10 mu; and F being conversion units necessary to produce an answer in foot-lamberts per nautical mile. The value was computed to be

$$_{A}B_{*}(0,90^{\circ},90^{\circ}) = 12.97 \text{ Foot-lamberts/nautical mile.}$$

$_{A}B_{*}(z,90^{\circ},90^{\circ})$ was determined for 20,000 feet altitude by Eq. 3.

$$_{A}B_{*}(20000,90^{\circ},90^{\circ}) = {}_{A}B_{*}(0,90^{\circ},90^{\circ})\ e^{-\frac{20000}{30000}}$$

and, because Fig. 5 is a semi-logarithmic plot, $e^{-z/30,000}$ plots as a straight line between the two end points $_{A}B_{*}(0,90^{\circ},90^{\circ}) = 12.97$ foot lamberts/nautical mile and $_{A}B_{*}(20,000,90^{\circ},90^{\circ}) = 6.67$ foot lamberts/nautical mile.

Measured Path Function vs Altitude. Next was plotted the measured $B_{*}(z,90^{\circ},90^{\circ})$. The difference between the measured B_{*} and the $_{A}B_{*}$ (computed for pure, dry air) is the effect of liquid water in suspension, and to a lesser degree, industrial haze, smoke particles, or any other material in suspension.

Relative Humidity vs Altitude. Also on Fig. 5 there is a plot of relative humidity. The only difference between the plots of relative humidity in Figs. 4 and 5 is the choice of horizontal coordinates, being linear in Fig. 4 and logarithmic in Fig. 5. The similarity between path function and relative humidity profiles is easily seen.

Path Function Not Affected by Water Vapor. Now the path function as measured does not indicate the presence of water vapor. Rayleigh scattering is defined as the scattering from very small particles including the molecules of air.[9] The atmosphere is made up of air, i.e., approximately 75.5% nitrogen, 23.15% oxygen, 1.28% argon, traces of other gases, and water vapor and liquid water in varying amounts.[1] If we postulate a dry atmosphere, i.e., one of nitrogen, oxygen, argon, and traces of other gases, and to this we add water vapor, each water vapor molecule must displace a gas molecule in order that the pressure remain the same. Then any increases of scattering due to water vapor can be computed as follows:

The total scattering function for Rayleigh scattering from gas molecules given by Johnson[11] as "scattering coefficient" is

$$\alpha(o) = \frac{32\pi^3}{3N\lambda^4}(m-1)^2 \qquad (4)^*$$

where N is the number of scatterers, λ the wavelength of light, and m the index of refraction of the gas.

The indices of refraction at standard atmospheric pressure and 0°C of N_2, O_2, and H_2O vapor are, respectively, 1.000249 to 1.000259, 1.000271, and 1.000296 to 1.000298[6]. The maximum possible increase due to water vapor would be when H_2O molecules displaced N_2 molecules and this increase

---

* Eq. 4 applies to gas at standard atmospheric pressure, i.e., at sea level, hence $s(z) = s(o)$.

would be

$$\frac{(m-1)^2_{H_2O}}{(m-1)^2_{N_2}} = \frac{(1.000298-1)^2}{(1.000249-1)^2} = 1.43$$

or 43 percent. But at standard atmospheric pressure of 1013.25 mb. and temperature of 15°C, the water vapor pressure is 17 mb. or 1.6 percent of the total pressure. Because the partial pressures of a mixture of gases is proportional to the numbers of molecules of the gases in the mixture the H_2O molecules would be 1.6 percent of the total molecules in the gas. This means that if all of the water vapor molecules introduced into the gas displaced only nitrogen molecules, the increase of total scattering function due to the water vapor would be .43 X .016 = .00688, i.e., 0.7 of 1 percent. This precision cannot be achieved in the attenuation meter by which path function is measured.

Liquid Water Indicated by Measured Path Function. The path function does indicate the presence of liquid water or other scattering material in the atmosphere. The preceding paragraph dealt with molecular scattering only, i.e., pure, dry air. According to Fritz[7] the atmosphere is never pure nor dry, but dust and water vapor are always present in varying degrees. van de Hulst[16] states that the scattering coefficient for Rayleigh molecular scattering varies as a function of λ^{-4}, and the scattering coefficient has been found to increase with increasing humidity. He further states that this increase is larger than that caused by molecular scattering of water vapor and that some of the molecules form small droplets or clusters of molecules. Junge,[12] reporting Wall, makes the following distinction between different types of nuclei:

(1) Particles insoluble in water and unwettable. These may serve as nuclei of condensation, but to do so require a large amount of super saturation. Their importance for the natural aerosol is slight.

(2) Particles insoluble in water, but wettable.

(3) Droplets of solution.

From certain evidence Junge[12] states that it appears that in the atmosphere there is a preponderance of droplets of solution.

The particles in the air vary in size from 10^{-6} to 10^{-1} cm. The size range from 10^{-6} to 10^{-1} cm covers two general classes of particles, "small" and "large," i.e., those having diameters of 10^{-5} cm or smaller which cause Rayleigh scattering, and those having diameters larger than 10^{-5} cm which cause Mie scattering. These particles, both "small" and "large," cause increase in path function over that due to molecular scattering only.

The total scattering function for Rayleigh scattering, i.e., small particles, but larger than molecules, is given by the following equation:[11]

$$A(0) = 24\pi^3 N \left(\frac{n^2-1}{n^2+2}\right)^2 \frac{V^2}{\lambda^4} \qquad (5)$$

where N is the number of scatterers, n is the index of refraction of the scattering medium (for water, n = 1.33), V is the volume of the scatterers, and λ is the wavelength of light. The total scattering function for Mie scattering is given by the same equation modified as follows:[11]

$$\alpha(0) = 24\pi^3 N \left(\frac{n^2-1}{n^2+2}\right)^2 \frac{V^2}{\lambda^4}\left[1 + \frac{6\pi^4}{5}\left(\frac{n^2-1}{n^2+2}\right)\frac{a^4}{\lambda^4}\cdots\right] \quad (6)$$

From these two equations it can be seen that the scattering coefficient varies directly as the number of scatterers, the square of the volumes of the scatterers, and, when the particles are "large," as the series enclosed in the brackets.

Molecular Scattering vs Particle Scattering. A comparison between the scattering coefficients for pure, dry air, i.e., molecular scattering, and for very small particle Rayleigh scattering follows:

(1) For molecular scattering, Eq. 4 is used, which may be rewritten as follows:

$$\alpha(0) = \frac{32}{3N}(m-1)^2 \frac{\pi^3}{\lambda^4}$$

Let m be a weighted average of the indices of refraction for 75 percent nitrogen and 25 oxygen equal to 1.000262; N is Loschmidt's number, 2.687×10^{19}, the number of molecules per cm^3 of an ideal gas at standard atmospheric pressure and $0^\circ C$.[13] Then, for molecular scattering, the total scattering function is

$$\alpha(0) = 2.73 \times 10^{-26} \frac{\pi^3}{\lambda^4}$$

(2) For Rayleigh scattering, Eq. 5 is used, and may be rewritten as follows:

$$\alpha(0) = 24N \left(\frac{n^2-1}{n^2+2}\right)^2 V^2 \frac{\pi^3}{\lambda^4}$$

Let n be 1.33, the index of refraction of water; V, the volume of one small particle having a radius of 10^{-6} cm, equal to $4/3\ \pi \times 10^{-18}$ cm^3; and N = 1. Then, for Rayleigh scattering by one small particle, the total scattering function is

$$\beta(0) = 1.78 \times 10^{-35} \frac{\pi^3}{\lambda^4}$$

To compare the above total scattering function with the total scattering function for molecular scattering, it is multiplied by 2.687×10^{19}, Loschmidt's number, so that there are the same number of scatterers per unit volume, in this case, cm^3, then

$$\beta(0) = 4.78 \times 10^{-16} \frac{\pi^3}{\lambda^4}$$

and the ratio of total scattering functions, particle to molecular, is

$$\frac{4.78 \times 10^{-16}}{2.73 \times 10^{-26}} \doteq 2 \times 10^{10}$$

Thus any small water particle that displaces an air molecule or is added to a volume of pure, dry air will, under any circumstances, increase the scattering. And, conversely, any increase in path function over the value due to molecular scattering is due to particles which are predominately liquid water. This discussion is not intended to be construed as saying that liquid water and liquid water alone is necessarily the sole cause of the scattering increase as indicated by a path function measurement, for there is always the possibility that non-hygroscopic particles may be present.

Microwave Refractive Modulus Independent of Liquid Water. The microwave refractometer when properly calibrated measures the microwave refractive modulus, N, directly. The microwave refractive modulus is a function of three variables, viz., temperature, total atmospheric pressure, and the partial pressure of water vapor present in the atmosphere.[2] There is some disagreement concerning the effect of liquid water on the operation of the microwave refractometer, but according to Enenstein[5] there is some effect. Cunningham, Plank, and Campen[3] find that the effect of liquid water, using Enenstein's equation is approximately 0.6N units for clouds, 0.5N units for rain, maximum, this is less than 1 percent of a typical value of atmospheric microwave refractive modulus. Inasmuch as the data presented in this paper were recorded for clear, i.e., cloud free weather, the effect of liquid water is negligible. Thus the relative humidity profile is valid.

Correlation Between Path Function and Relative Humidity. Correlation between the path function and relative humidity profiles was made by the following steps:

(1) The difference between the measured path function and the path function for pure, dry air, i.e., the effect of liquid water and other materials in suspension, was tabulated for each 100 feet. This is ${}_{p}B_{*}(0,90^{\circ},90^{\circ})$

(2) The above differences were normalized at the maximum value.

(3) The normalized path function ${}_{p}B_{*}$ values were plotted vertically against the relative humidity values plotted horizontally. This is Fig. 6.

RESULTS

In general Fig. 6 shows that with high relative humidity values, above 80 percent, small changes of relative humidity are accompanied by large changes in path function; that with low relative humidity values, below 60 percent, large changes of relative humidity are accompanied by small changes of path function; and from 65 percent relative humidity to 85 percent relative humidity another relationship exists.

Discussion. Middleton[15] states that there is comparatively little change in the radii of liquid droplets with changes of relative humidity below about 70 percent, and Fig. 6 tends to bear this out. The plot of relative humidity values from 67 percent to 85 percent and $_{P}B_{*}$ values of .22 and .35 seem to be anomalous in that it forms a reverse curve.

The data plotted in Fig. 6 were recorded in two airplanes flying several hundreds of feet apart, with the refractometer equipped airplane flying slightly behind and higher than the B-29. Thus it would appear that the data might be affected by the airplane flying through inhomogeneous aerosol, i.e., through different moisture cells. The effect from this would more than likely be of a random nature, while the plot of the reverse curve in Fig. 6 does not show randomness.

All of the data plotted in Fig. 6 were recorded while flying over the Atlantic Ocean in the vicinity of Patrick Air Force Base. It is of interest that the data in question, i.e., the reverse curve plot,

were the data recorded from 2000 feet altitude down to 1000 feet altitude. Woodcock and Gifford as reported by Junge[12] deposited haze droplets on small glass plates and showed that over the ocean practically all these droplets consists of NaCl solutions. And Simpson and Wall, again as reported by Junge[12], have pointed out that in the case of crystallization of NaCl from droplets the size of droplets is bound tc decrease in a discontinuous manner until all water is evaporated. It is possible that some such process is responsible for the apparent discontinuity in Fig. 6.

Recently a microwave refractometer was installed in the Visibility Laboratory equipped B-29 with its probe located within two feet of the attenuation meter by which path function is measured. It is expected that data from future flights will show less deviation than that reported herein, and it is expected that it can be determined whether the reverse curve is a real effect or not.

ACKNOWLEDGEMENTS

The assistance by different groups and persons who, through their efforts, has made this research program possible is acknowledged. While thanks are due to all contributors to this effort, special mention is made of:

Air Force Cambridge Research Center Test Support Group who furnished B-29 and crew;

Aircraft Commander, Capt. Robert L. Baron, USAF, who by his understanding of the work at hand contributed many worthwhile suggestions;

M/Sgt. Robert C. Harbig, Engineer, and S/Sgt. Philip H. Knights, crew chief, who kept the airplane always ready for flight; and

Mr. Tom Obst, office of Range Development, Patrick Air Force Base, Florida, who arranged for the refractometer equipped C-131 to accompany the B-29 on this flight.

REFERENCES

1. Berry, F. A. Jr., E. Bollay, and N. R. Beers, Handbook of Meteorology, McGraw-Hill, New York, pp. 351 and 373, (1945).

2. Crain, C. M., and J. R. Gerhardt, "Some Preliminary Studies of the Rapid Variations in the Index of Refraction of Atmospheric Air at Microwave Frequencies," Bulletin of the American Meteorological Society, 31, pp. 330-331 (1950).

3. Cunningham, R. M., V. G. Plank, and C. F. Campen, Jr., "Cloud Refractive Index Studies," Geophysical Research Papers, No. 51, Air Force Cambridge Research Center, p. 2, (1956).

4. Duntley, S. Q., A. R. Boileau, and R. W. Preisendorfer, "Image Transmission by the Troposphere I, "Journal of the Optical Society of America, 47, pp. 499-506, (1957).

5. Enenstein, N. H., "The Effect of Water Droplets on the Index of Refraction," Proceedings, Symposium on Tropospheric Wave Propogation, U. S. Navy Electronics Laboratory Report No. 173, p. 52, (1948).

6. Eshbach, O. W., Handbook of Engineering Fundamentals, John Wiley and Sons, New York, P. 9-15. (1949).

7. Fritz, Sigmund, "Solar Radiant Energy and its Modifications by the Earth and its Atmosphere," Compendium of Meteorology, American Meteorological Society, Boston, p. 23, (1951).

8. Haltiner, G. J., and Frank L. Martin, Dynamical and Physical Meteorology. McGraw-Hill, New York, pp. 23-24, (1957).

9. International Dictionary of Physics and Electronics, Walter C. Michels, Senior Editor, Van Nostrand Co., New York, p. 804, (1956).

10. Johnson, Francis S., "The Solar Constant," Journal of Meteorology, 11, pp. 431-439, (1954).

11. Johnson, John C., Physical Meteorology, M.I.T. Tech. Press and John Wiley and Sons, New York, pp. 33-44, (1954).

12. Junge, C., "Nuclei of Atmospheric Condensation," Compendium of Meteorology, American Meteorological Society, Boston, p. 188, (1951).

13. Middleton, W.E.K., Vision Through the Atmosphere, Univ. of Toronto Press, Toronto, pp. 20-24 (1952).

14. Preisendorfer, R. W., Theory of Attenuation Measurements in Planetary Atmospheres, SIO Ref. 58-81. Scripps Institution of Oceanography, University of California, La Jolla, Calif., 24 Nov 1958.

15. Tousey, R., and E. O. Hulburt, "Brightness and Polarization of the Daylight Sky at Various Altitudes above Sea Level," Journal of the Optical Society of America, 37, pp. 78-92, (1947).

16. Van de Hulst, H. C. The Atmosphere of Earth and Planets, edited by C. P. Kuiper, Univ. of Chicago Press, Chicago, pp. 55-56 (1948).

ARB:deg
1/10/59

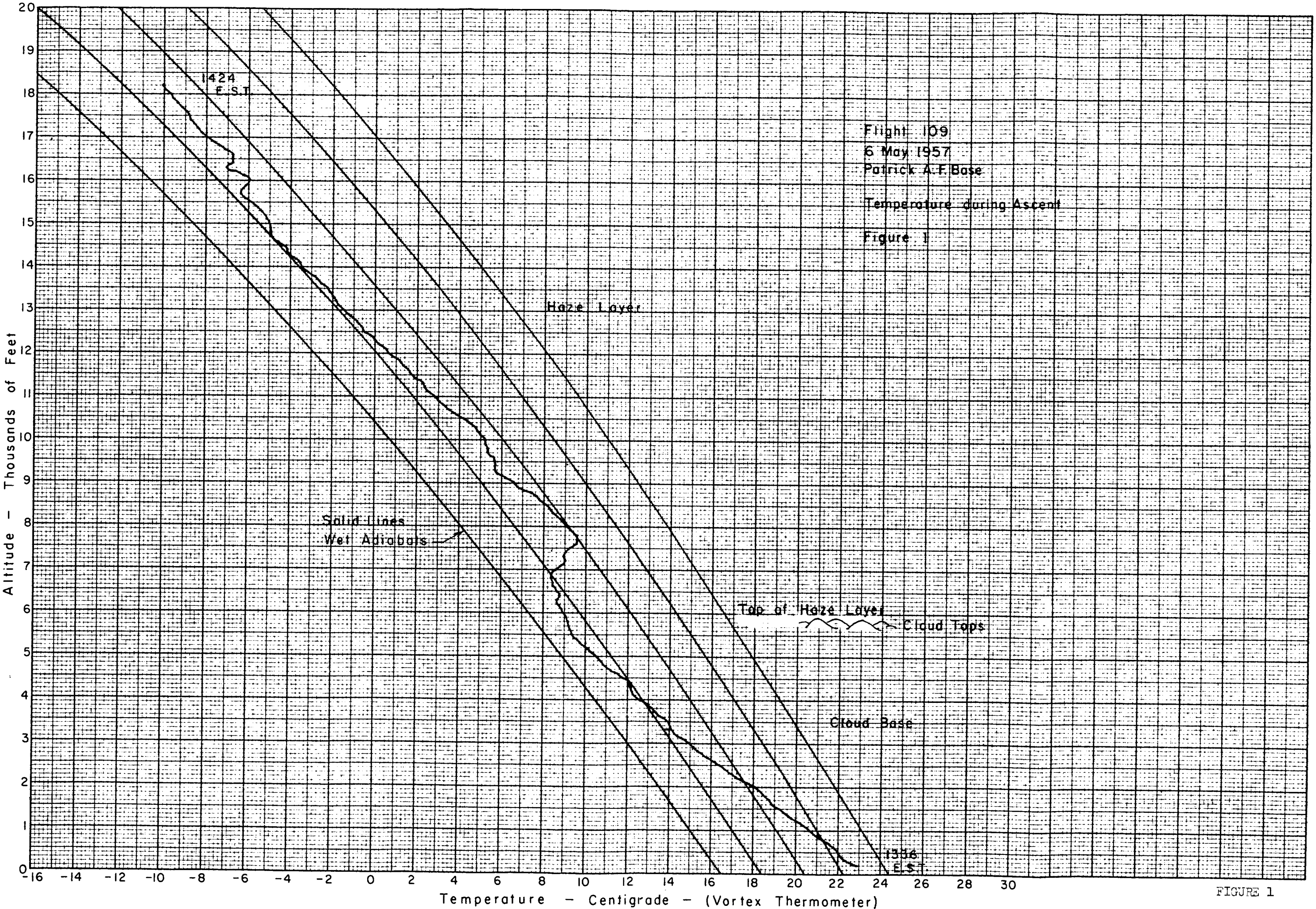
1424
E.S.T.
Haze Layer
Flight 109
6 May 1957
Patrick A.F. Base
Temperature during Ascent
Figure 1
Solid Lines
Wet Adiabats
Top of Haze Layer
Cloud Tops
Cloud Base
1336
E.S.T.
Altitude - Thousands of Feet
Temperature - Centigrade - (Vortex Thermometer)
20
19
18
17
16
15
14
13
12
11
10
9
8
7
6
5
4
3
2
1
0
-16
-14
-12
-10
-8
-6
-4
-2
0
2
4
6
8
10
12
14
16
18
20
22
24
26
28
30

FIGURE 1

Flight 109
6 May 1957
Patrick A.F. Base

Temperature during Descent

Figure 2

1436 E.S.T.

1451 E.S.T.

1501 E.S.T.

1509 E.S.T.

Solid Lines
Wet Adiabats

Altitude — Thousands of Feet

Temperature — Centigrade — (Vortex Thermometer)

FIGURE 2

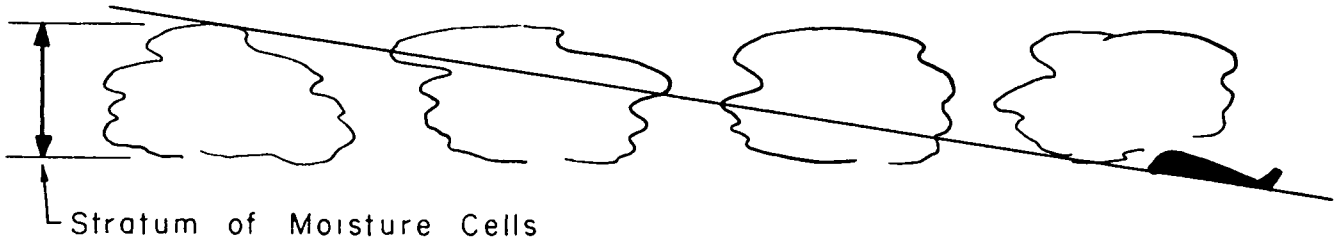

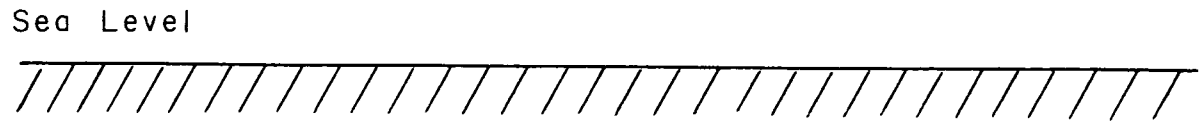

Figure 3

Flight 109
6 May 1957
Patrick A.F. Base

Formation Flight B-29 (725) and
Microwave Refractometer - Equipped C-131

Debye Equation $N = \frac{77.6p}{T} + \frac{77.6 \times 4810\, e}{T^2}$

p. = Total Pressure, Millibars

e = Partial Pressure of Water Vapor, Millibars

T = Absolute Temperature

$N = (n-1)\,10^6$

n = Refractive Index of Air

Figure 4

1436 E.S.T.

1501 E.S.T.

1510 E.S.T.

$N_{e=e_s} = \frac{77.6p}{T} + \frac{77.6 \times 4810\, e_s}{T^2}$

$N_{e=0} = \frac{77.6p}{T}$

N Recorded

Microwave Refractive Modulus vs Altitude

Altitude – Thousands of Feet

N Number

150 160 170 180 190 200 210 220 230 240 250 260 270 280 290 300 310 320 330 340 350

1436 E.S.T.

1501 E.S.T.

1510 E.S.T.

Relative Humidity vs Altitude

Altitude – Thousands of Feet

.1 .2 .3 .4 .5 .6 .7 .8 .9 1.0

e/e_s

0 1 2 3 4 5 6 7 8 9 10 11 12 13 14 15 16 17 18

FIGURE 4

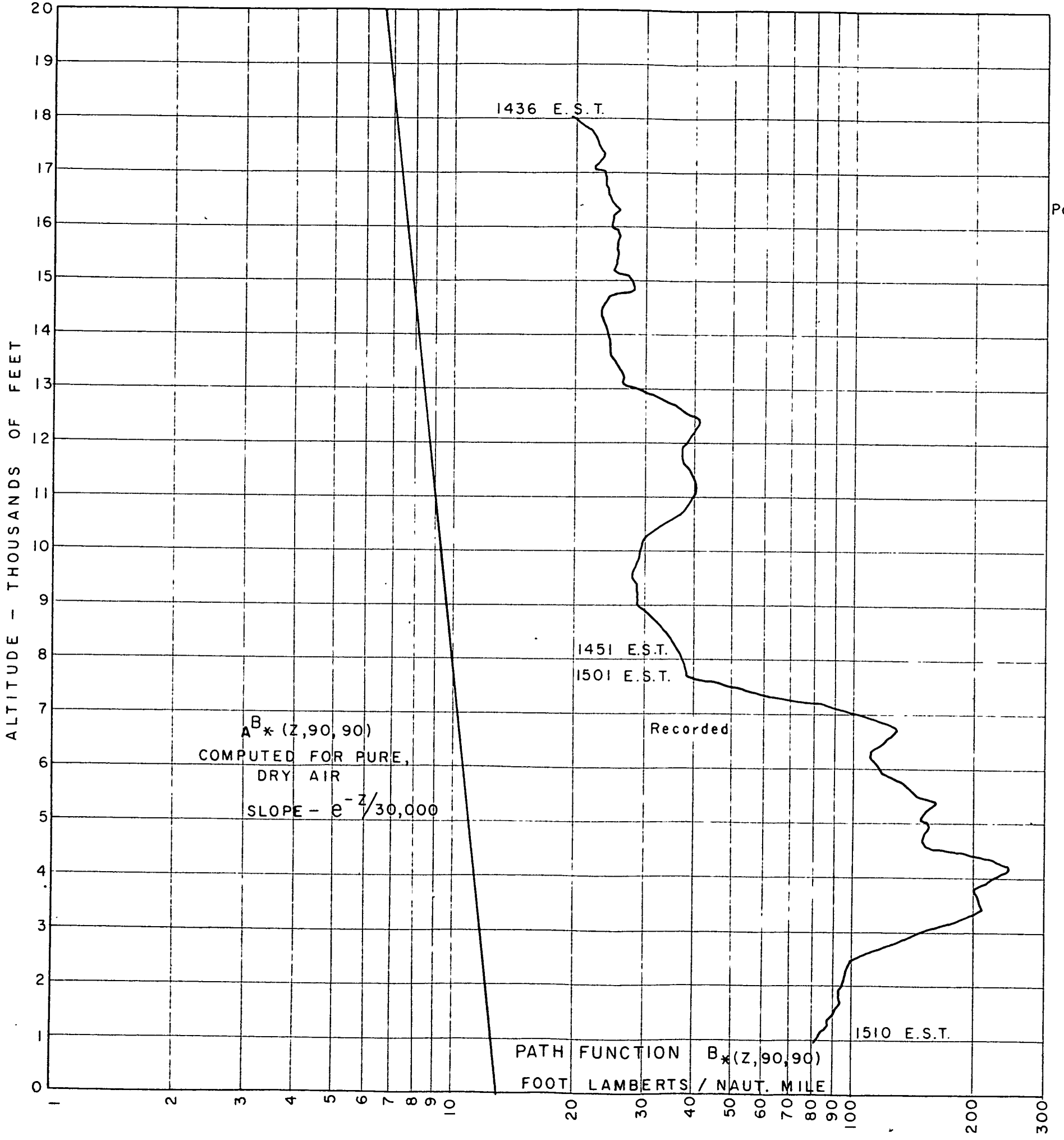

Flight 109
6 May 1957
Patrick A.F. Base

Figure 5

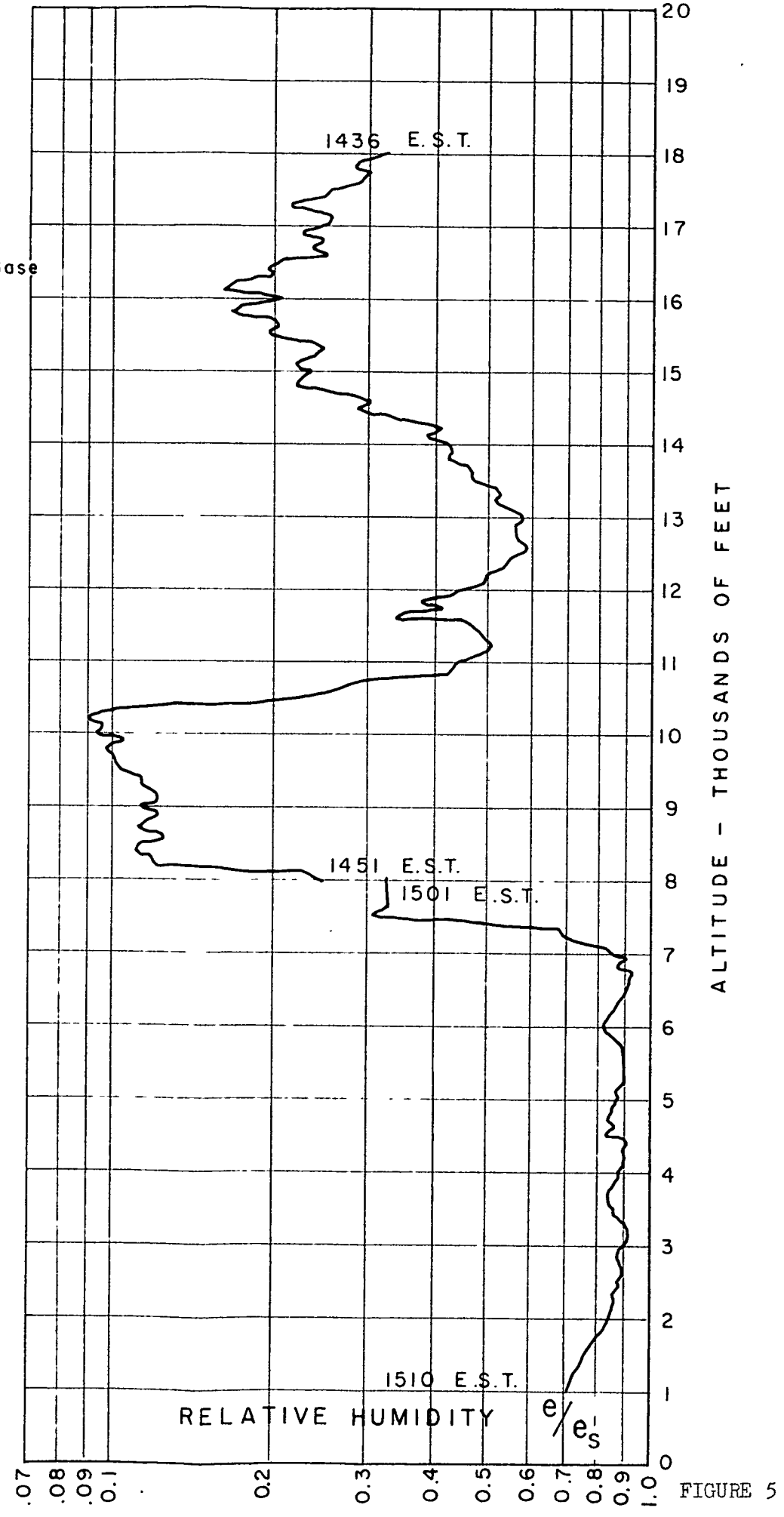

FIGURE 5

FLIGHT 109
6 MAY 1957
PATRICK A. F. BASE
FIGURE 6